



# Combined solar power and storage as cost-competitive and grid-compatible supply for China's future carbon-neutral electricity system

Xi Lu<sup>a,b,c,1,2</sup>, Shi Chen<sup>a,d,1</sup>, Chris P. Nielsen<sup>d</sup>, Chongyu Zhang<sup>a</sup>, Jiacong Li<sup>a</sup>, He Xu<sup>e</sup>, Ye Wu<sup>a,c</sup>, Shuxiao Wang<sup>a</sup>, Feng Song<sup>f</sup>, Chu Wei<sup>f</sup>, Kebin He<sup>a,b</sup>, Michael B. McElroy<sup>d,g,2</sup>, and Jiming Hao<sup>a,c</sup>

<sup>a</sup>School of Environment, State Key Joint Laboratory of Environment Simulation and Pollution Control, Tsinghua University, Beijing 100084, China; <sup>b</sup>Institute for Carbon Neutrality, Tsinghua University, Beijing 100084, China; <sup>c</sup>Beijing Laboratory of Environmental Frontier Technologies, Tsinghua University, Beijing 100084, China; <sup>d</sup>Harvard John A. Paulson School of Engineering and Applied Sciences, Harvard University, Cambridge, MA 02138; <sup>e</sup>College of Environmental Science and Engineering, Nankai University, Tianjin 300350, China; <sup>f</sup>School of Applied Economics, Renmin University of China, Beijing 100872, China; and <sup>g</sup>Department of Earth and Planetary Sciences, Harvard University, Cambridge, MA 02138

Edited by Gunnar Luderer, Potsdam Institute for Climate Impact Research, Potsdam, Germany, and accepted by Editorial Board Member Hans J. Schellnhuber August 30, 2021 (received for review February 24, 2021)

**As the world's largest CO<sub>2</sub> emitter, China's ability to decarbonize its energy system strongly affects the prospect of achieving the 1.5 °C limit in global, average surface-temperature rise. Understanding technically feasible, cost-competitive, and grid-compatible solar photovoltaic (PV) power potentials spatiotemporally is critical for China's future energy pathway. This study develops an integrated model to evaluate the spatiotemporal evolution of the technology-economic-grid PV potentials in China during 2020 to 2060 under the assumption of continued cost degression in line with the trends of the past decade. The model considers the spatialized technical constraints, up-to-date economic parameters, and dynamic hourly interactions with the power grid. In contrast to the PV production of 0.26 PWh in 2020, results suggest that China's technical potential will increase from 99.2 PWh in 2020 to 146.1 PWh in 2060 along with technical advances, and the national average power price could decrease from 4.9 to 0.4 US cents/kWh during the same period. About 78.6% (79.7 PWh) of China's technical potential will realize price parity to coal-fired power in 2021, with price parity achieved nationwide by 2023. The cost advantage of solar PV allows for coupling with storage to generate cost-competitive and grid-compatible electricity. The combined systems potentially could supply 7.2 PWh of grid-compatible electricity in 2060 to meet 43.2% of the country's electricity demand at a price below 2.5 US cents/kWh. The findings highlight a crucial energy transition point, not only for China but for other countries, at which combined solar power and storage systems become a cheaper alternative to coal-fired electricity and a more grid-compatible option.**

solar photovoltaic power | electricity potential | economic competitiveness | solar plus storage

Coal has been the dominant energy source fueling the swift growth of China's economy over the past 40 y. Primary energy consumption in China increased by a factor greater than 8.5 from 1978 to 2019, while the fraction of coal in the energy supply declined only modestly, from 66.8 to 57.6%, over the same time period (1). China is responsible now for ~28.8% of the total CO<sub>2</sub> emissions worldwide, nearly twice that of the United States, the world's second largest emitter (1). Due largely to the same reasons, severe air pollution episodes have occurred frequently over central and eastern regions of China, where the vast majority of its population is concentrated (2). China pledged to peak its carbon emissions by at least 2030 and achieve carbon neutrality by 2060 during the United Nations General Assembly in 2020 (3). Decarbonization of the energy system is recognized as a priority for China to address the intertwined challenges of domestic air pollution and global climate change (4). One of the biggest challenges facing China is to deploy low- or zero-carbon power generation capacity to meet the increased demand for electricity and

to substitute for existing coal-fired capacity in the longer term (5, 6). Among alternative sources, solar photovoltaic (PV) power generation is expected to play an important role in this process in China given abundant solar resources and huge PV manufacturing capacity (7–10).

The global capacity of solar PV generation has nearly tripled over the last half decade, increasing from 304.3 GW in 2016 to 760.4 GW in 2020 (11, 12). Solar power has been the fastest growing power source globally, comprising 50% of global investment in renewable energy from 2010 to 2019 and ranking first in net added generation capacity (13). The top 10 countries in terms of new installations in 2020, together totaling 78% of the global market, included 6 in the Asia-Pacific region (China, India, Japan, Vietnam, Australia, and Korea), 2 in Europe (Germany and the Netherlands), and 2 in the Americas (Brazil and the United States). China retained the leading position in terms of total installed capacity, accounting for almost one-third of the global total (12).

## Significance

Solar photovoltaic power is gaining momentum as a solution to intertwined air pollution and climate challenges in China, driven by declining capital costs and increasing technical efficiencies. The dynamic spatial trajectory of cost-competitive and grid-compatible penetration potentials for solar power will be a critical determinant of the speed of energy system decarbonization in China. This study develops an integrated model to assess solar photovoltaic potentials and their cost competitiveness throughout 2020 to 2060 considering multiple spatiotemporal factors. We find that the cost competitiveness of solar power allows for pairing with storage capacity to supply 7.2 PWh of grid-compatible electricity, meeting 43.2% of China's demand in 2060 at a price lower than 2.5 US cents/kWh.

Author contributions: X.L., S.C., M.B.M., and J.H. designed research; X.L. and S.C. performed research; X.L., S.C., C.Z., J.L., H.X., Y.W., S.W., F.S., C.W. and K.H. contributed new analytic tools; X.L., S.C., and C.P.N. analyzed data; and X.L., S.C., C.P.N., M.B.M., and J.H. wrote the paper.

The authors declare no competing interest.

This article is a PNAS Direct Submission. G.L. is a guest editor invited by the Editorial Board.

This open access article is distributed under [Creative Commons Attribution-NonCommercial-NoDerivatives License 4.0 \(CC BY-NC-ND\)](https://creativecommons.org/licenses/by-nc-nd/4.0/).

See [online](#) for related content such as Commentaries.

<sup>1</sup>X.L. and S.C. contributed equally to this work.

<sup>2</sup>To whom correspondence may be addressed. Email: xilu@tsinghua.edu.cn or mbm@seas.harvard.edu.

This article contains supporting information online at <https://www.pnas.org/lookup/suppl/doi:10.1073/pnas.2103471118/-DCSupplemental>.

Published October 11, 2021.

The rocketing growth of solar PV in China started with the introduction in 2011 of a nationwide incentive policy of feed-in tariffs (14). With its total installed capacity of solar PV surpassing that of the United States in 2013 and Germany in 2015 (15, 16), China has maintained its leading global position in terms of not only the deployment of solar power but also the manufacture of PV modules. With addition of 48.2 GW in 2020, China's installed capacity of solar PV rose to 253.4 GW (12), far ahead of a target of 105 GW set for 2020 in the 13th 5-y plan (17).

The large-scale installation of solar power both globally and in China has promoted improvements in PV conversion efficiencies and reductions in generation costs. Capital costs of utility-scale solar PV per kW fell by 63.3% between 2011 and 2018 in China, accompanied by a number of downward adjustments in the levels of subsidies (18). With the advantage of the lowered cost, solar is expected to play a key role in the future power system. Previous studies have discussed the economic competitiveness of solar power in China at city or provincial levels, but these analyses either were static snapshots of the solar industry in individual or several discrete years or failed to capture the spatial differences across the nation (19–21). From a power-system perspective, many large-scale simulations for China have projected the solar PV capacity shares in the future (22–24). However, the role of solar PV in future energy systems is often underestimated with high capital cost assumptions, which did not fully reflect the recent cost decline trend of the solar PV (25–27). The stepwise deployment of large-scale solar capacity (23, 28, 29) requires in-depth research of the spatiotemporal characteristics of solar potentials from technical and economic perspectives. In addition, the cost reduction of solar power, and similar trends in storage technologies like lithium-ion batteries (28), brings an opportunity to integrate storage systems into solar power stations. Such combined systems would be able not only to generate cost-competitive electricity but also bring additional benefits to balance solar variability and better meet demand. According to the 2019 to 2020 Energy Storage Action Plan jointly issued by the National Energy Administration and three other related ministries in China (30), the application of energy storage technology will be promoted in coordination with utility-scale renewable power generation. And provinces including Shandong, Shanxi, Xinjiang, Henan, and Inner Mongolia have explicitly required newly built solar power stations to pair with storage capacity (31). For a dynamic and quantitative understanding of these prospects, it is imperative to know precisely when, where, and to what extent subsidy-free solar PV power plus

storage may be not only technically feasible and cost competitive but also grid compatible.

In this study, we developed an integrated technical, economic, and grid-compatible solar resource assessment model to analyze the spatial distribution and temporal evolution of the cost competitiveness of utility-scale solar power and its viable grid penetration potential in China from 2020 to 2060. Solar radiation and temperature data were derived from the Goddard Earth Observing System Forward Processing Version 5 (GEOS-5 FP) of the Data Assimilation System with a spatial resolution of 0.25° latitude by 0.3125° longitude and a temporal resolution of 1 h (32). The study adopted the assimilation data for a continuous 6-y interval from 2014 to 2019 to generate hourly technical potentials that account for the interannual variability of solar radiation and temperature, with spatial distribution calibrated by the long-term yearly average data from Global Solar Atlas (33). The technical potential of utility-scale solar PV was evaluated with consideration of multiple factors including resource endowment, topographical and land-use constraints, latitude-dependent PV configurations, and time-varying efficiency factors, following the approach described by Chen et al. (34). Building on this, the prices and the dynamic cost-competitive parity potential of solar PV power were modeled spatially across China over the study period tuned with the up-to-date economic parameters. In addition, the grid penetration potentials of the solar-plus-storage systems were further quantified spatiotemporally for China through the integration of the techno-economic model and an hourly power dispatch model.

## Results

**Technical Potential.** The total annual technical potential of solar PV generation is estimated to be as high as 99.2 PWh in 2020, equivalent to ~13.2 times the electricity demand for China in the same year, and corresponding to a potential generating capacity of 64.3 TW. The capacity factor of this potential, that is, the projected unit electricity output divided by the nameplate maximum output, is estimated to be 17.6% on average. The generating potential is estimated to increase to 118.2 PWh in 2030 and 146.1 PWh in 2060, responding to improvements in conversion efficiency and system performance. With an increasingly important role for electricity in meeting future growth in energy end uses, electricity demand in China is projected to grow to 16.7 PWh in 2060, more than doubling the demand in 2018 (35). Should 50% of the incremental demand for electricity in 2060 relative to 2020 be met by solar PV power, it would require roughly 2,871 GW of

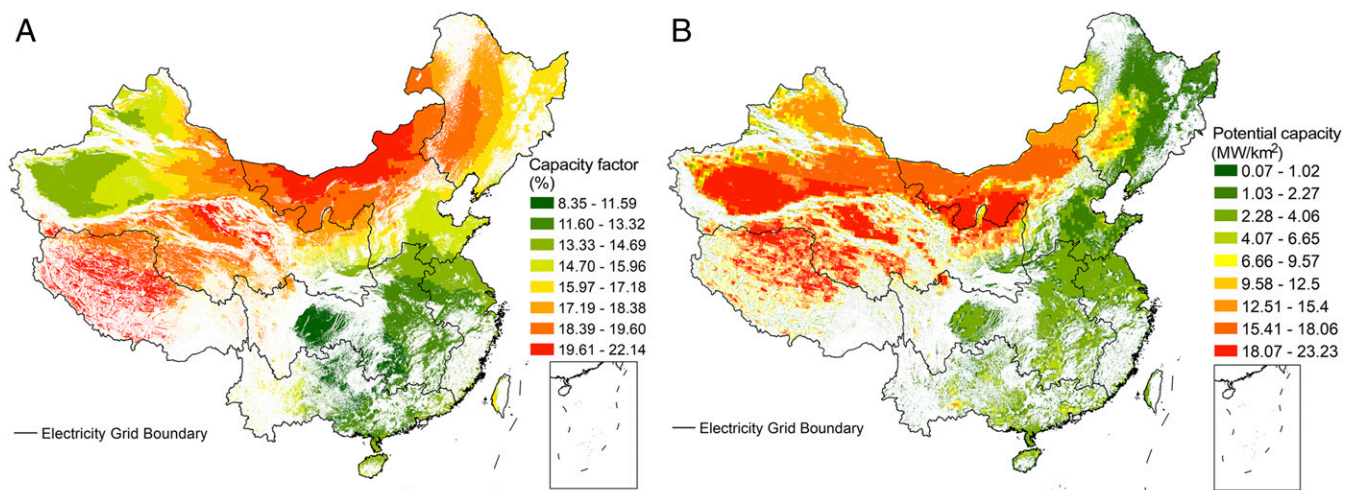


**Fig. 1.** Distribution of technical potentials of utility-scale solar PV of China in 2020. (A) Distribution of capacity factors by grid cell. (B) Distribution of potential capacity expressed in megawatts per square kilometer.

installed capacity assuming the national average capacity factor, accounting for 4.5% of the total technical potential capacity in 2020. There is great variation in regional solar generating potential reflecting multiple influences, including solar resources, land availability, and latitude-dependent installation densities. The solar PV potentials of Tibet and the three northern power grids in 2020, including the Northwest, North China, and Northeast grids, exceed their respective total regional generation by more than a factor of 12 (reference *SI Appendix, Fig. S1* for the grid and provincial potential distribution). By contrast, the potential of solar PV to serve power demand in southern power grids is relatively low, especially for the East China grid, which accounts for 20.7% of national electricity demand, 18.9% of the population, and 27.5% of gross domestic product. The capacity factors and potential capacity show similar spatial distributions (Fig. 1 *A* and *B*), which indicate that the regions with larger available areas and installation densities per unit land area also tend to have greater solar resources. The top five provinces with the highest potential capacities include Xinjiang, Inner Mongolia, Tibet, Qinghai, and Gansu, each with a potential capacity higher than 3.6 TW. The total potential capacity of these provinces reaches 54.9 TW in 2020, accounting for 85.4% of the national potential capacity. The regions with the highest capacity factors are concentrated in the Qinghai-Tibet Plateau, Gansu, Ningxia, and Inner Mongolia, in contrast to the lowest capacity factors, in southeast China.

A large share of the early development of solar power in China occurred in the above-mentioned favorable areas. For example, the newly installed capacities of Xinjiang and Gansu, two northwestern provinces, alone accounted for 50.8% of the national total in 2013 (36). Solar power stations in these provinces suffer from high curtailment rates due primarily to short-term overcapacity relative to local electric power demand. The curtailment rates in Xinjiang and Gansu reached as high as 32.2 and 30.5%, respectively, in 2016 (37). In contrast, solar PV power initially developed slowly in China's central and eastern regions. Driven by a combination of limited capacity to integrate variable solar power into the local power systems of the western region and air pollution control policies that increasingly constrain coal use in eastern China, there has been an evident west-to-east shift of solar PV

development in China. By the end of 2020, the share of national solar PV capacity installed in the Northwest grid had declined to 24%, while the share in the East China and Central China grids had increased to 19 and 13%, respectively (38).

**Economic Parity Potential.** Bus-bar prices denote the lowest power selling prices acceptable for solar power stations under reasonable expectations for profit (*Materials and Methods*). The geographic distribution of calculated solar bus-bar prices for 2020 features low values in the west and north and high values in the east and south (Fig. 2*A*). The arithmetic national average bus-bar price in China is 0.34 CNY(Chinese yuan)/kWh (4.93 US cents/kWh, expressed in 2019 currency, the same below), with the Tibet grid displaying the lowest bus-bar price across the country at 0.29 CNY/kWh (4.20 US cents/kWh) and Central China the highest, averaging 0.43 CNY/kWh (6.23 US cents/kWh). And the population-weighted national average bus-bar price in the same year reaches 0.40 CNY/kWh (5.80 US cents/kWh) due to the mismatch of solar resource and population distribution (reference *SI Appendix, Fig. S2* for national average price from 2020 to 2060). Fig. 2*B* further shows the distribution of economic potentials varying with the bus-bar price for each regional grid in 2020. There is greater total economic potential at given bus-bar prices in low-priced regions due to the greater areal share of resource-favorable conditions. The low-priced potential is concentrated in the Tibet and Northwest grids, reflecting the higher capacity factors of solar power in these resource-abundant regions. The bimodal distribution for the Northwest reflects the differential solar resources of Qinghai (located mainly on the Tibetan Plateau) versus other northwest provinces. High-priced potentials are seen in the East China, South China, and Central China grids, where the solar radiation resource is inferior to that in the inland regions.

The temporal evolution of spatial cost competitiveness between solar and coal is shown in Fig. 3. Supply curves in Fig. 3*A* show the temporal evolution of the relationship between electricity prices and the corresponding economically viable solar potential. The curves move downward from 2020 to 2060 due primarily to the rapidly decreasing costs of capital driven by the reduced costs of PV modules, balance of system (BOS), and operation and maintenance (O&M), along with an improvement in efficiencies for

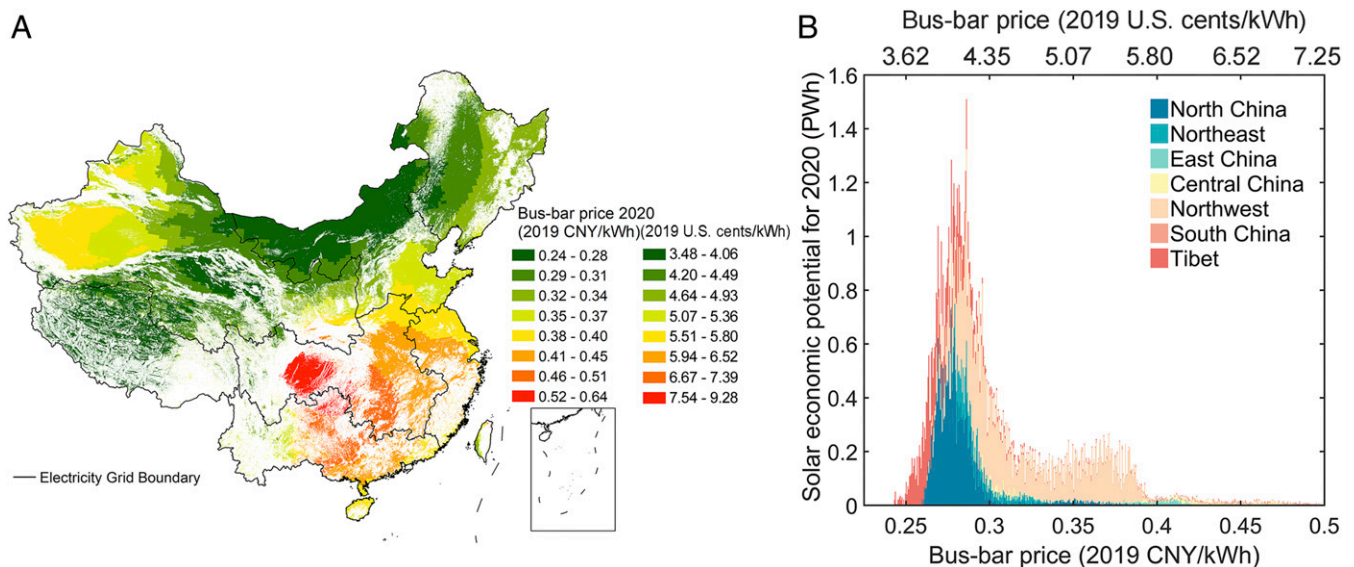


**Fig. 2.** Spatial distribution of the solar power price and economic potential in China. (A) Distribution of the utility-scale solar bus-bar prices in 2020. All bus-bar prices in the study are expressed in 2019 CNY and US cents according to the 2019 exchange rate of 6.9:1 (CNY:USD). (B) Distribution of solar potentials by bus-bar price in 2020. The color and height of the bars indicate the source grids of the solar potential and the amounts of available economic potential, respectively.

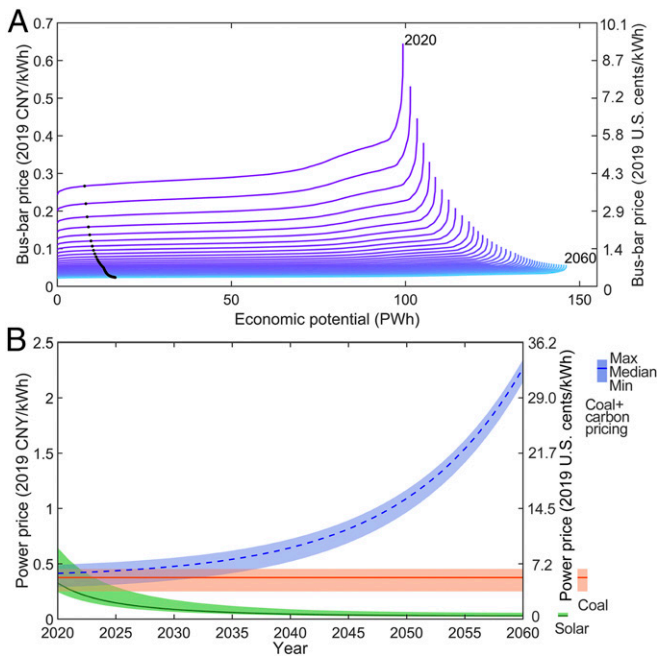


**Fig. 3.** Temporal evolution of the solar power economic competitiveness in China. (A) The supply curves of China's utility-scale solar PV for 2020 to 2060. The abscissa of the black point on each curve represents the predicted electricity generation in the corresponding year, and the ordinate corresponds to the lowest solar PV bus-bar price required to meet the generation demand. (B) Evolution of national prices of solar PV, coal power, and coal power plus carbon pricing.

conversion of solar energy to electricity. The national average bus-bar price in China is expected to decline to 0.09 CNY/kWh (1.30 US cents/kWh) and 0.03 CNY/kWh (0.43 US cents/kWh) in 2030 and 2060, respectively. The rate of decrease will gradually decline. In addition, the supply curves flatten out over time, implying that the spatial differences in solar bus-bar prices across the country will narrow in the future. The maximum bus-bar prices, at which the solar potential equals the total electricity demand projected for given years, shows a fast-declining tendency from 0.27 CNY/kWh (3.91 US cents/kWh) in 2020 to 0.07 CNY/kWh (1.01 US cents/kWh) in 2030, and 0.02 CNY/kWh (0.29 US cents/kWh) in 2060 (black dots in the Fig. 3A).

The bus-bar prices of solar PV are generally compared with the on-grid electricity tariffs for coal power, a benchmark price at which coal-fired plants sell electricity to the grid companies, to

determine whether solar power stations need subsidies (39) (reference *SI Appendix, Fig. S3* for the local coal power tariffs distribution). Fig. 3B illustrates the temporal evolution of national solar PV bus-bar prices versus coal power on-grid tariffs between 2020 and 2060. The ranges of the price curves reflect primarily their spatial differences. As of 2021, 78.6% of the potential capacity, or 79.7 PWh, has already reached parity compared to local coal power tariffs. It should be emphasized that the externalities of coal power, including the health damages of air pollution and other environmental costs, are not priced in the tariffs (40). If the externalities were included, solar power would be even more competitive (Fig. 3B). The year when the solar power price is lower than the local on-grid tariffs for coal power is defined as the parity year. Nationwide parity is estimated to be achieved by 2023. Solar power in the North China, Northeast, East China, and Tibet grids is projected to achieve full price parity with coal in 2021, followed by the Central China, Northwest, and South China grids in 2023 (reference *SI Appendix, Fig. S4* for the spatial distribution of the parity year).

The total potential of solar power that achieves a cost-competitive bus-bar price compared to coal-fired power is defined as the parity potential. The ratio of solar parity potential relative to total technical potential is referred to as the parity ratio. In 2020, the parity ratios for the East China, Central China, and South China grids reach more than 33.1% despite of the relative lower solar radiation resource, in contrast to the ratio of 37.0% for the Northwest grid. The enhanced competitiveness of solar power relative to coal in eastern regions is attributed to higher costs for generation of coal-fired electricity in these regions. With the rising competitiveness of renewables such as solar in the electricity market, coupled with the weak growth in demand for coal power plants, carbon emission costs and more stringent environmental regulations, the capacity factors of coal power plants may be expected to continue their recent decline, resulting in an expected increase in coal power cost (41). This in turn will further enhance the relative competitiveness of solar and accelerate its substitution for coal in the power market. Should a carbon price of 45 CNY/ton (6.5 USD [US Dollar]/ton)  $\text{CO}_2$  be implemented in China in 2020 and rise rapidly up to 2,251 CNY/ton (326.2 USD/ton)  $\text{CO}_2$  in 2060 (reference *SI Appendix, Fig. S5* for the carbon price projections), as suggested as a means to achieve China's carbon neutrality target (42), the achievement of nationwide price parity would be advanced to 2022. And the national parity ratios in the years of 2020 and 2021 will increase from 63.9 to 91.1% and from 78.6 to 98.0%, respectively. As shown in the Fig. 3B, the cost advantage of solar power over coal power will be further amplified with anticipated carbon pricing mechanisms in the long term.

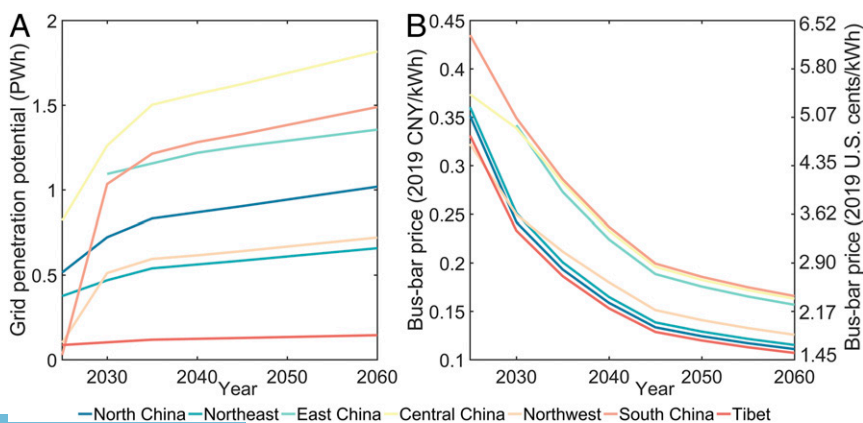


**Fig. 4.** The grid penetration potential (A) and bus-bar prices of solar-plus-storage systems (B) in seven regional electric grids of China from 2025 to 2060.

**Grid Penetration Potential.** The declining cost of solar power leaves more room for investments in the pairing of solar generation with electricity storage to address the variation challenges for grid integration. The costs of some forms of storage are declining similarly to those of solar PV, for example, an 80% decline in the cost of lithium-ion batteries over the last 8 y (28). In 2019, lithium-ion batteries account for 76.1 and 56.3% of the newly installed storage capacity of the world and China, respectively (43). With little requirement for geographical conditions, significant technological advantages and economies of scale across multiple industries, the lithium-ion batteries have been a promising storage choice to be combined with solar power stations (44, 45). This study further investigated the spatiotemporal cost-competitive and grid-compatible grid penetration potential when solar is equipped with 100% equivalent storage capacity. The penetration potential of the combined system in the future Chinese electricity system was optimized for each grid region on an hourly basis from 2020 to 2060 at 5-y intervals to serve demand in the most grid-compatible manner. Specifically, under the constraints of avoiding curtailment and generating electricity at cost equal to or lower than coal power, the optimization target was to minimize the variability of the remaining net demand after absorbing the power supply from the combined system. The parameters assumed for the storage system and detailed optimization settings are described in *Materials and Methods*.

Results suggest that the grid penetration potential for the solar-plus-storage system increases from 5.2 PWh in 2030 to 7.2 PWh in 2060. As shown in Fig. 4A, the grid penetration potential of solar power is highest for Central China and lowest for Tibet, estimated at 1.8 PWh and 0.1 PWh, respectively, for 2060. The unbalanced distribution of the grid penetration potentials highlights the importance of transregional cooperation to better utilize solar potentials in regions with relatively low demand. In contrast, the highest grid penetration potential for solar power systems without storage is 2.2 PWh nationally in 2030 and 3.2 PWh in 2060. An increase of 4 PWh in the grid penetration potential in 2060 results from the introduction of the storage systems. The national average bus-bar price required to achieve the grid penetration potential decreases from 0.25 CNY/kWh (3.62 US cents/kWh) in 2030 to 0.12 CNY/kWh (1.74 US cents/kWh) in 2060. As indicated in the Fig. 4B, highest bus-bar price is observed in the South China grid at 0.17 CNY/kWh (2.46 US cents/kWh) in 2060, while lowest bus-bar price exists in the Tibet grid at 0.11 CNY/kWh (1.59 US cents/kWh).

In addition, the combined system exhibits better compatibility with demand. The hourly optimization results for the Northwest and East China grids are shown in Fig. 5. The results indicate that, without added storage, an extreme ramping-up requirement for other power sources appears after sunset, and the net load variability after the integration of solar power (expressed as the average of the absolute values of the hourly ramp up/down rate) increases by 421.8% for the Northwest grid and 56.4% for the East China grid compared to the original load variability, as shown in Fig. 5A and B. After incorporating the storage systems, the net load variability is greatly reduced, by 47.0 and 82.0%, respectively, for Northwest and East China compared to the solar-only system (Fig. 5C and D). The storage system tends to store surplus solar power at midday and discharge it toward evening or early morning to better serve the surges in demand. The regular charge–discharge diurnal cycle of the storage system decreases the turnover rate of the battery and thus potentially enlarges the application of the combined system.

## Discussion

Here, we developed and applied an integrated approach to evaluate the economic competitiveness and the potentials of subsidy-free solar PV power generation with combined storage systems in China, including systematic consideration of temporal and spatial factors. At present, subsidy-free solar power has become cheaper

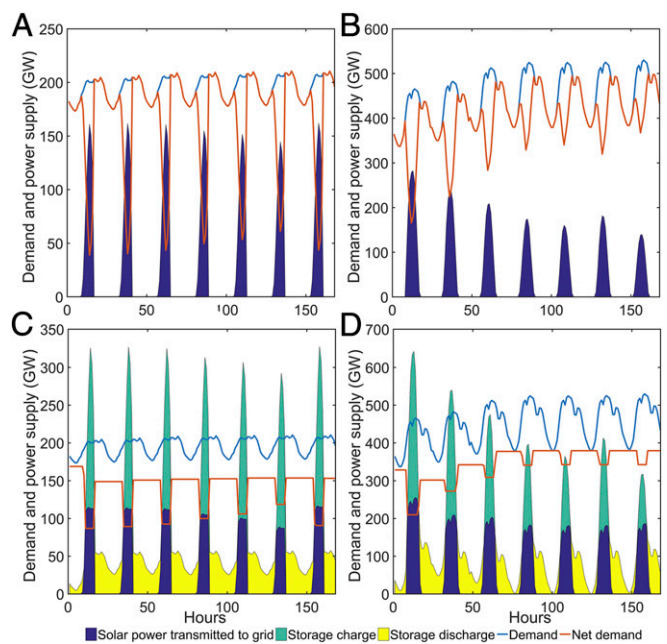


**Fig. 5.** Hourly dispatch to achieve the maximum penetration of grid-compatible and cost-competitive solar in the first week of January 2060. (A) Hourly demand and solar supply for the Northwest grid using solar power generation without storage. (B) The same as A but for the East China grid. (C) The same as A but using solar-plus-storage systems. (D) The same as B but using solar-plus-storage systems.

than coal power in most parts of China, and this cost-competitive advantage will soon be further enhanced and extended spatially due to technology advances and cost declines. Our results demonstrate that the economic competitiveness of solar power combined with investments in storage systems could provide extra benefits for grid dispatch, which will be especially important for operation of future electric systems in China. The findings of this analysis may capture a critical point in energy transition not only for China but many other countries in mid and low latitudes, where solar-plus-storage systems can serve as a carbon-neutral, cost-competitive, grid-compatible alternative option to coal-fired power generation.

Sensitivity analysis was conducted to evaluate the relative importance of the parameters affecting the solar power price and the grid penetration potential (*Materials and Methods*). The results show that the system performance coefficient, the discount rate, the debt ratio of the capital structure, and the ratio of O&M to capital investment are the most sensitive variables in determining bus-bar prices (*SI Appendix, Fig. S6 and Table S1*). These factors invite attention in order to further reduce bus-bar prices for solar power. The future large-scale adoption of advanced technologies including bifacial modules and one- and two-axis tracking systems may also provide opportunities for further cost reductions. In addition, possible fluctuation of future storage costs within a somewhat wider range may affect the bus-bar prices of the solar-plus-storage systems. Under a scenario assuming lower storage system costs (*SI Appendix, Fig. S7*), the national average bus-bar price will decline from 0.12 CNY/kWh (1.74 US cents/kWh) to 0.09 CNY/kWh (1.30 US cents/kWh) in 2060 (reference *SI Appendix, Table S2* for the sensitivity analysis results by regional grid). In contrast, it could increase to 0.16 CNY/kWh (2.32 US cents/kWh) under a scenario of high storage system costs (*SI Appendix, Fig. S7*). This invites further efforts to speed up and scale up application of storage in all fields thus to accelerate the reduction in costs.

Realizing the penetration potentials (7.2 PWh) of the solar-plus-storage systems in the future power grid corresponds to a

10.8 TWh installed capacity of the lithium-ion batteries storage systems in 2060. Assuming the lifespan of the batteries storage system is half of that of the PV power generation system, and a 99% recycle efficiency of the key metals lithium, nickel, and cobalt and 98% efficiency of manganese, the cumulative metals needed to realize the step-by-step ambition equal to 1.4, 6.4, 2.5, and 3.2 Mt, respectively (46), equivalent to 8.0, 7.2, 36.3, and 0.4% of the world reserve (47). To lessen rare metals scarcity challenges requires promoting alternative materials, especially for cobalt, and realizing the echelon use of the batteries across multiple sectors like transportation. Moreover, continuous efforts have to be made to advance the efficiency and energy density, cycle of charge-discharge, and lifespan of the batteries in order to reduce the requirement for materials and mitigate the life-cycle environmental impacts at the same time (48–50).

The results of the study suggest that solar plus storage could serve as a cost-competitive and grid-compatible source for a carbon neutrality power system in China. It should be mentioned here that the interaction of the combined solar and storage system with the other components in the power system is not taken into consideration. In the renewables-dominant future power system of China, the precise match of supply and demand will require coordinated regulating of the storage facilities from the supply, grid, and demand aspects. On the supply side, hydropower and pumped hydropower storage would also serve as storage capacities especially for southwest regions in China. Concentrating solar power is another low-carbon alternative with storage capacities despite the current higher costs. On the demand side, electrification of more end-use sectors like transportation is beginning to reduce other forms of energy use while also providing greater load flexibility and storage capacities to compensate for the variability in production of renewables. On the grid side, specialized energy storage power stations will replace traditional thermal power plants to provide peak and frequency regulation functions and ensure the safety of the power grid operation. All the other choices could also help enhance the matching of demand with solar supply, potentially reducing the storage capacity needed in the solar-plus-storage system. In this case, the cost advantage of solar PV could be further amplified.

The decline in costs for solar power and storage systems offers opportunity for solar-plus-storage systems to serve as a cost-competitive source for the future energy system in China. The transportation, building, and industry sectors account, respectively, for 15.3, 18.3, and 66.3% of final energy consumption in China (5). If costs continue to decline, such as the opportunity for power storage, applications to use solar PV electricity to power vehicles (in forms of either electricity or electrolytic hydrogen), to heat or cool buildings through heat pumps, and to produce chemical industrial products (such as ammonia and methane) may extend the climate and environmental benefits of solar energy far beyond the traditional power-generating and -consuming sectors currently emphasized.

## Materials and Methods

**Installation Capacity Potential.** Areas suitable for utility-scale solar PV were identified with consideration of natural constraints including slope and land-use type. Areas with slopes larger than 5% were excluded (34). For remaining areas, suitability factors ranging from 0 to 20% were allocated to each land-use category (SI Appendix, Table S3). A solar PV array model was developed assuming the fixed tilt configuration and south-facing orientation and applying hourly GEOS-5 FP solar radiation data from 2014 to 2019, calibrated by the long-term yearly average data from Global Solar Atlas (33). The latitude-dependent tilt of solar PV modules was determined through a linear curve fitting derived from the optimal PV tilt layouts determined empirically at 360 representative sites in 31 provinces in mainland China (SI Appendix, Fig. S8) (51). The spacing between footprints of neighboring PV modules was determined using the solar altitude angle at 3 PM on the winter solstice in order to avoid shade for most of the daytime throughout the year. The packing factor, defined by the ratio of the effective module area to the required land

area, can be evaluated according to particular settings of tilt and module spacing. The nominal power per unit area of solar module was quantified from 2020 to 2060 assuming increasing efficiency of conversion of solar radiation to electricity. The national potential installed capacity (kW) in the year  $t$  (2020 to 2060) was aggregated spatially:

$$CP_t = \sum_{j=1}^m \left( \sum_{i=1}^n s_{i,j} \times sf_i \right) \times PF_j \times P_{wp,t} \div 1,000, \quad [1]$$

where  $m$  denotes the total number of data grid cells in China;  $n$  denotes the land-use suitability category ( $n = 7$ );  $s_{i,j}$  indicates the suitable area of land-use type  $i$  in grid cell  $j$  after accounting for the slope constraints ( $m^2$ );  $sf_i$  is the suitability factor of land-use type  $i$  shown in SI Appendix, Table S3;  $PF_j$  denotes the packing factor of grid cell  $j$ ;  $P_{wp,t}$  is the nominal power per unit area of PV module ( $W/m^2$ ) in the year  $t$  under standard test conditions (cell temperature of 25 °C and radiation of 1,000  $W/m^2$  with an air mass 1.5 [AM1.5] spectrum).

The equations used to calculate tilt, spacing, packing factor, and nominal power per unit area of PV module are listed in SI Appendix, section 1.

**Electricity Generation Potential.** The hourly solar radiation available to PV modules in each location was evaluated in direct beam, diffuse, and reflected radiation categories, respectively. Input parameters included horizontal surface direct beam solar radiation, diffuse radiation, tilt, solar altitude angle, and solar azimuth angle for each daytime hour of the year. The three types of radiation were then summed to obtain the total available for PV conversion to electricity. The influence of ambient temperature on output was assessed using temperatures derived from GEOS-5 on an hourly basis. The influence of shading on electricity output was modeled hourly, based on the PV array model and the position of the sun in the sky. Dynamic increases of the PV conversion efficiency and the system performance coefficient (used to further evaluate the reliability of the system operation and the efficiency of the system components) were taken into account annually for the study period of 2020 to 2060 (SI Appendix, section 1). The solar generation potential (kWh) in the year  $t$  (2020 to 2060) was calculated by the following:

$$GP_t = \sum_{k=1}^h \left( \sum_{j=1}^m \left( \sum_{i=1}^n s_{i,j} \times sf_i \right) \times P_{k,j,t} \right) \div 1,000, \quad [2]$$

where  $h$  denotes the total number of hours in the year  $t$ ;  $P_{k,j,t}$  denotes hourly generation potential per unit land area ( $W/m^2$ ) of grid cell  $j$  in hour  $k$  in the year  $t$ . Other variables in the equation are defined in Eq. 1.

The equations used to calculate the system performance coefficient, radiation (direct beam, diffuse, and reflected) reaching the PV module, temperature correction coefficient, shading correction coefficient, and hourly generation potential are listed in SI Appendix, section 1.

**Initial Capital Costs.** The capital costs of a utility-scale PV solar power farm can be broken down into two parts, namely the costs of PV modules and those for the BOS. The BOS refers to everything needed aside from PV modules to make the solar station functional, which includes inverters, fixed support, combiner boxes, cables, and other items. To accurately characterize the declining trend of capital costs for solar power projects in China, we applied the learning curve method for the modules and BOS separately (SI Appendix, Fig. S9).

The learning curve for PV modules can be expressed as follows:

$$C_t = C_0 \left( \frac{N_t}{N_0} \right)^{-\alpha}, \quad [3]$$

where  $N_t$  represents the installed capacity of solar modules in the year  $t$ ;  $N_0$  is the initial installed capacity;  $C_t$  is the solar module cost in the year  $t$ ;  $C_0$  is the initial solar module cost; and  $\alpha$  is the learning index.  $\alpha$  was estimated to be 0.80 using continuous data for solar module prices in China and for solar module capacities installed from 2007 to 2019 (SI Appendix, Table S4) (52). Following similar estimation methods for the PV modules, the learning index for BOS was evaluated in this study as 0.57.

The costs of PV modules and BOS in the year  $t$  were determined based on the estimation for solar installed capacity in the future (44), with detailed information presented in SI Appendix, section 2.

**Bus-Bar Prices.** A net present value (NPV) method was adopted in this study to calculate the bus-bar prices of utility-scale solar power farms. The bus-bar price denotes the lowest electricity price required by utility-scale solar PV farms to obtain a specified internal rate of return. The NPV model was applied for

each grid cell from 2020 to 2060 to generate a dynamic spatial distribution of bus-bar prices. Cash flows for each year were discounted to the beginning of the construction year at a given discount rate and added to yield the NPV. The bus-bar price was the electricity price under the condition at which NPV equals zero.

Specifically, the NPV can be expressed as follows:

$$NPV = \sum_{t=0}^n \frac{CF_t}{(1+rd)^t} \quad [4]$$

where  $CF_t$  refers to the cash flow in year  $t$ ;  $n$  is the lifetime of the utility-scale solar PV project ( $n = 26$ );  $rd$  refers to discount rate; and  $t = 0$  represents the construction period.  $CF_t$  can be calculated by the following:

$$CF_t = R_t + L_t - KC_t + RV_t - LP_t - OM_t - T_t, \quad [5]$$

where  $R_t$  refers to annual revenue,  $L_t$  refers to inflow of loan funds,  $RV_t$  refers to residual value of fixed assets,  $KC_t$  refers to initial capital costs (SI Appendix, Fig. S9),  $LP_t$  refers to repayment of the loan and interest,  $OM_t$  refers to costs of O&M, and  $T_t$  denotes payment of taxes.

The setting of parameters for the economic model was based on a survey on solar PV projects in Shanxi, Hebei, and Inner Mongolia in China (SI Appendix, Table S5). The construction period was assumed to be one year and the operational period 25 y. The debt ratio of the capital structure was assumed to be 70%. The loan funds and the interest during the construction period were repaid based on an equivalent annuity over the first 15 y of operations. The interest during the construction period was selected here as 1% of the total capital expenditures. The decrease of PV module efficiency due to natural degradation with prolonged usage was assumed at 3% in the first operational year and 0.7% for the following operational years. The residual values were assumed to be 5% of the fixed assets with linear depreciation. The annual interest rate was assumed to be 5.5%. The discount rate was assumed to be 8%. The rates for value-added tax, enterprise income tax, and combined sales tax and extra charges were assumed be 17, 25, and 11%, respectively. The annual O&M cost per watt was assumed to be 1% of the total capital expenditures per watt (19). The equations used to calculate the cash flow are included in SI Appendix, section 2.

**Solar-Plus-Storage Dispatch Model.** The storage system is assumed to be integrated with the solar power station and will be replaced once in the middle of the operational lifespan of the power station. The power generation and storage capacity potential data used in the grid optimization model were aggregated from the grid cell to the regional power grid level with the constraints that the bus-bar price of the combined solar and storage system is equal to or lower than the coal power price. The calculation of the bus-bar price of the combined system is shown in Eq. 4, with the capital cost of the storage capacities included in the initial capital cost.

In the grid optimization model, the main decision variables include the following: hourly solar power generation directly connected to the grid  $P$ ; hourly battery charge  $P_c$ ; hourly battery discharge  $P_d$ ; and hourly state of charge of the battery  $SOC$ , which are constrained by the equations below:

$$SOC \geq SOC_{min}, \quad [6]$$

$$SOC \leq SOC_{max}, \quad [7]$$

$$SOC_{ith} = SOC_0, \quad [8]$$

$$P_{c,k} \geq 0, \quad [9]$$

$$P_{c,k} \leq P_r \times S_k, \quad [10]$$

$$P_{d,k} \geq 0, \quad [11]$$

$$P_{d,k} \leq P_r \times (1 - S_k), \quad [12]$$

$$0 \leq P_k \leq GP_k, \quad [13]$$

$$P_{c,k} + P_k = GP_k, \quad [14]$$

$$P_{d,k} + P_k \leq L_k, \quad [15]$$

$$SOC_1 = SOC_0 + P_{c,1} \times ec - P_{d,1}/ed, \quad [16]$$

$$SOC_k = SOC_{k-1} + P_{c,k} \times ec - P_{d,k}/ed \quad (k \geq 2), \quad [17]$$

where  $SOC_{min}$  and  $SOC_{max}$  denote the minimum and maximum states of charge, equal to 20 and 100% of the potential storage capacity in the unit of kWh, respectively;  $SOC_{ith}$  denotes the state of charge at the end of the modeling cycle;  $SOC_0$  the state of charge at the beginning of the cycle;  $P_r$  is the nominal power rating of the storage facilities in the unit of kW, and the duration time is 2 h in the analysis;  $GP_k$  the solar power generation in the hour  $k$ ;  $L_k$  the load in the hour  $k$ ;  $S_k$  is a binary variable indicating if the storage capacity is charged ( $S_k = 1$ ) or discharged ( $S_k = 0$ );  $ec$  the efficiency of charge (95%); and  $ed$  the efficiency of discharge (95%). The solar capacity and grid penetration potentials were optimized to realize the highest grid compatibility on an hourly basis. The optimization object of minimizing the net load variability was used to investigate the grid penetration potential of solar-plus-storage system to best serve demand, and the objective function was defined as the sum of the square of the net loads:

$$\min \sum (L_k - P_k - P_{d,k})^2. \quad [18]$$

**Sensitivity Analysis.** We applied Monte Carlo methods to evaluate the sensitivity of bus-bar prices in 2020 to key parameters, including learning rates for solar modules and BOS, O&M costs, annual interest rate, debt ratio of the capital structure, discount rate, and system performance coefficient. A uniform or normal distribution was selected for all of the above parameters as listed in SI Appendix, Table S1. The analysis was based on a grid cell with annual potential electricity generation of 459.1 GWh and potential capacity of 303.6 MW in 2020. The simulation was run 10,000 times. In addition, the impact of storage cost on the bus-bar prices of the combined systems was modeled under another two scenarios, one low cost (SI Appendix, Fig. S7) and one high cost (SI Appendix, Fig. S7). The results are shown in SI Appendix, Table S2.

**Data Availability.** All study data are included in the article and SI Appendix.

**ACKNOWLEDGMENTS.** This work was supported by the National Natural Science Foundation of China (Grants 72025401, 71974108, and 71690244), China Postdoctoral Science Foundation Grant BX2021148, Shuimu Tsinghua Scholar Program 2021SM014, the Tsinghua University-Inditex Sustainable Development Fund, and grants from the Office of the President of Harvard University and the Harvard Global Institute to the Harvard-China Project on Energy, Economy and Environment.

- BP Public Limited Company, Statistical review of world energy 2020 (2020).
- M. Li et al., Study on population distribution pattern at the county level of China. *Sustainability* **10**, 3598 (2018).
- S. Mallapaty, How China could be carbon neutral by mid-century. *Nature* **586**, 482–483 (2020).
- Boston Consulting Group, *China climate pathways report* (BCG, Beijing, 2020).
- China Electric Power Planning & Engineering Institute, *China Energy Development Report 2018* (EPPEI, Beijing, 2019).
- The Climate Group, *RE100: China's Fast Track to a Renewable Future* (RE100, China, 2015).
- W. Liu, H. Lund, B. V. Mathiesen, X. Zhang, Potential of renewable energy systems in China. *Appl. Energy* **88**, 518–525 (2011).
- D. Zhang et al., Present situation and future prospect of renewable energy in China. *Renew. Sustain. Energy Rev.* **76**, 865–871 (2017).

- X. Ruhang, Characteristics and prospective of China's PV development route: Based on data of world PV industry 2000–2010. *Renew. Sustain. Energy Rev.* **56**, 1032–1043 (2016).
- G. He et al., SWITCH-China: A systems approach to decarbonizing China's power system. *Environ. Sci. Technol.* **50**, 5467–5473 (2016).
- International Energy Agency, *Trends in PV applications 2019* (IEA-PVPS, Paris, 2020).
- International Energy Agency, *2020 Snapshot of Global PV Markets* (IEA, Paris, 2021).
- Frankfurt School UNEP Centre/BloombergNEF, Global trends in renewable energy investment 2019 (FS-UNEP Centre/BNEF, Germany, 2020).
- NDRC, *Notice on Improvement of the Electricity Price Policy for Solar Photovoltaic Power Generation* (National Development and Reform Commission of China, 2011).
- International Energy Agency, *2014 Snapshot of Global PV Markets* (IEA, Paris, 2015).
- International Energy Agency, *2015 Snapshot of Global PV Markets* (IEA, Paris, 2016).
- National Energy Administration, *13th Five Year Plan for Solar Energy* (NEA, Beijing, 2016).

18. China Renewable Energy Engineering Institute, *China Renewable Energy Development Report* (CREEI, Beijing, 2019).
19. J. Yan, Y. Yang, P. Elia Campana, J. He, City-level analysis of subsidy-free solar photovoltaic electricity price, profits and grid parity in China. *Nat. Energy* **4**, 709–717 (2019).
20. Y. Wang, S. Zhou, H. Huo, Cost and CO<sub>2</sub> reductions of solar photovoltaic power generation in China: Perspectives for 2020. *Renew. Sustain. Energy Rev.* **39**, 370–380 (2014).
21. M. Zhang, Q. Zhang, Grid parity analysis of distributed photovoltaic power generation in China. *Energy* **206**, 118165 (2020).
22. T. Burandt, B. Xiong, K. Löffler, P.-Y. Oei, Decarbonizing China's energy system—Modeling the transformation of the electricity, transportation, heat, and industrial sectors. *Appl. Energy* **255**, 113820 (2019).
23. D. Bogdanov et al., Arising role of photovoltaic and wind energy in the power sector and beyond: Changing the Northeast Asian power landscape. *Jap. J. Appl. Phys.* **57**, 08RJ01-1-08RJ01-10 (2018).
24. G. He et al., Rapid cost decrease of renewables and storage accelerates the decarbonization of China's power system. *Nat. Commun.* **11**, 2486 (2020).
25. M. Jaxa-Rozen, E. Trutnevyte, Sources of uncertainty in long-term global scenarios of solar photovoltaic technology. *Nat. Clim. Chang.* **11**, 266–273 (2021).
26. M. Xiao, T. Junne, J. Haas, M. Klein, Plummeting costs of renewables—Are energy scenarios lagging? *Energy Strategy Rev.* **35**, 100636 (2021).
27. M. Victoria et al., Solar photovoltaics is ready to power a sustainable future. *Joule* **5**, 1041–1056 (2021).
28. N. M. Haegel et al., Terawatt-scale photovoltaics: Transform global energy. *Science* **364**, 836–838 (2019).
29. E. Vartiainen, G. Masson, C. Breyer, D. Moser, E. Román Medina, Impact of weighted average cost of capital, capital expenditure, and other parameters on future utility-scale PV levelised cost of electricity. *Prog. Photovolt. Res. Appl.* **28**, 439–453 (2019).
30. National Energy Administration, *Energy Storage Action Plan 2019-2020 Jointly Issued by Four Ministries* (National Energy Administration, 2019).
31. S. Wang, Which provinces have specified the allocation of energy storage for photovoltaic projects during the 14th Five-Year Plan? <http://www.escn.com.cn/news/show-1137301.html>. Accessed 15 December 2020.
32. Global Modeling and Assimilation Office, *File Specification for GEOS-5 FP (Forward Processing)* (GMAO, 2013).
33. World Bank Group, *Global Solar Atlas version 2.0* (Solargis, Slovakia, 2021).
34. S. Chen et al., The potential of photovoltaics to power the Belt and Road Initiative. *Joule* **3**, 1895–1912 (2019).
35. CNPC Economics & Technology Research Institute, *China Energy Outlook 2050* (CNPC ETRI, Tokyo, 2017).
36. National Energy Administration, *Photovoltaic Power Generation Statistics of 2013* (NEA, Beijing, 2014).
37. National Energy Administration, *Report on the Operation and Grid Connection of Renewable Energy in Northwest Region in 2016* (NEA, Beijing, 2017).
38. China Renewable Energy Monitoring Center, *Installed capacity and power generation of wind and solar power across the country in 2020* (CREMC, Beijing, 2021).
39. J. Yuan et al., Deregulation of power generation planning and elimination of coal power subsidy in China. *Util. Policy* **57**, 1–15 (2019).
40. International Monetary Fund, *Global fossil fuel subsidies remain large: An update based on country-level estimates* (IMF, Washington, D.C., 2019).
41. C. Zhao et al., The economics of coal power generation in China. *Energy Policy* **105**, 1–9 (2017).
42. X. Zhang, *Scenario analysis of low-carbon energy transition under the 2060 carbon neutral target* (Institute of Energy, Environment and Economy of Tsinghua University, Beijing, 2021).
43. China Center for Information Industry Development, “White paper on the development of energy storage industry under the vision of carbon neutrality in China” (CCID, Beijing, 2021). <https://www.ccidgroup.com/info/1105/32718.htm>. Accessed 24 September 2021.
44. International Renewable Energy Agency, *Future of Solar Photovoltaic* (IRENA, Abu Dhabi, 2019).
45. International Renewable Energy Agency, *Electricity storage and renewables: Costs and markets to 2030* (IRENA, Abu Dhabi, 2017).
46. International Energy Agency, *Global EV outlook 2018* (IEA, Paris, 2019).
47. U.S. Geological Survey, *Mineral commodity summaries 2020* (USGS, Virginia, 2021).
48. A. Abdon et al., Techno-economic and environmental assessment of stationary electricity storage technologies for different time scales. *Energy* **139**, 1173–1187 (2017).
49. A. R. Dehghani-Sanj, E. Tharumalingam, M. B. Dusseault, R. Fraser, Study of energy storage systems and environmental challenges of batteries. *Renew. Sustain. Energy Rev.* **104**, 192–208 (2019).
50. L. Oliveira et al., Environmental performance of electricity storage systems for grid applications, a life cycle approach. *Energy Convers. Manage.* **101**, 326–335 (2015).
51. Solar Ofweek, Optimal panel tilt of utility-scale solar PV power station for 360 cities in China (2016). <https://solar.ofweek.com/2016-10/ART-260009-8300-30047659.html>. Accessed 12 December 2020.
52. International Energy Agency, *National survey report of PV power applications in China 2011-2019* (IEA-PVPS, Paris, 2019).

